arXiv:0805.4769v1 [nucl-ex] 30 May 2008

High-density QCD with CMS at the LHC

David d'Enterria for the CMS collaboration
CERN, CH-1211 Geneva 23, Switzerland

Abstract. The capabilities of the CMS experiment to explore the rich heavy-ion physics programme offered by the CERN Large Hadron Collider (LHC) are summarised. Various representative measurements in Pb-Pb collisions at $\sqrt{s_{NN}}$ = 5.5 TeV are covered. These include "bulk" observables – charged hadron multiplicity, low-p_T inclusive hadron spectra and elliptic flow – which provide information on the collective properties of the system; as well as perturbative processes – high-p_T hadrons, jets, γ-jet and quarkonium production – which yield "tomographic" information of the densest phases of the reaction.

Introduction

The prime goal of high-energy heavy-ion physics is to study the fundamental theory of the strong interaction – Quantum Chromodynamics (QCD) – in extreme conditions of temperature, density and parton momentum fraction (low-x). The collisions of lead nuclei at the LHC ($\sqrt{s_{NN}}$ = 5.5 TeV) will probe quark-gluon matter at unprecedented values of energy density. A detailed description of the potential of CMS to carry out a series of representative Pb-Pb measurements has been presented in [1]. We summarise this work here plus more recent developments [2]. Heavy-ion observables accessible to measurement with CMS include:

- "Soft" observables [3]: charged hadron multiplicity ($dN_{ch}/d\eta$), inclusive identified hadron spectra (dN/dp_T) and elliptic flow (v_2 parameter); which provide constraints on the collective properties (entropy density, viscosity, ...) of the produced strongly interacting medium.
- Perturbative probes [2, 4]: quarkonia, heavy-quarks, jets, γ-jet and high-p_T hadrons; which are produced very early in the collision, are potentially modified while traversing the medium, and thus yield "tomographic" information (colour density, $\langle\hat{q}\rangle$ transport coefficient, critical energy density, ...) of the hottest and densest phases of the reaction.

The LHC will open a new frontier in the study of QCD matter, thanks to the large energy densities attainable, $\varepsilon_{Bjorken} \approx 10$ GeV/fm^3 at initial times‡ τ_0 = 1 fm/c; the very low values of parton fractional momenta $x \approx p_T/\sqrt{s_{NN}}\,exp(-\eta) = O(10^{-5})$ accessible in the collision [5]; and the very abundant production of hard probes (with cross sections 10 to 10^4 larger than at RHIC, see Fig. 1).

‡ Notice that the "canonical" initial-time, τ_0 = 1 fm/c, is 200 times larger than the crossing-time of the two nuclei at LHC energies: $\tau_{cross} \approx 2R/\gamma \approx 5\,10^{-3}$ fm/c.

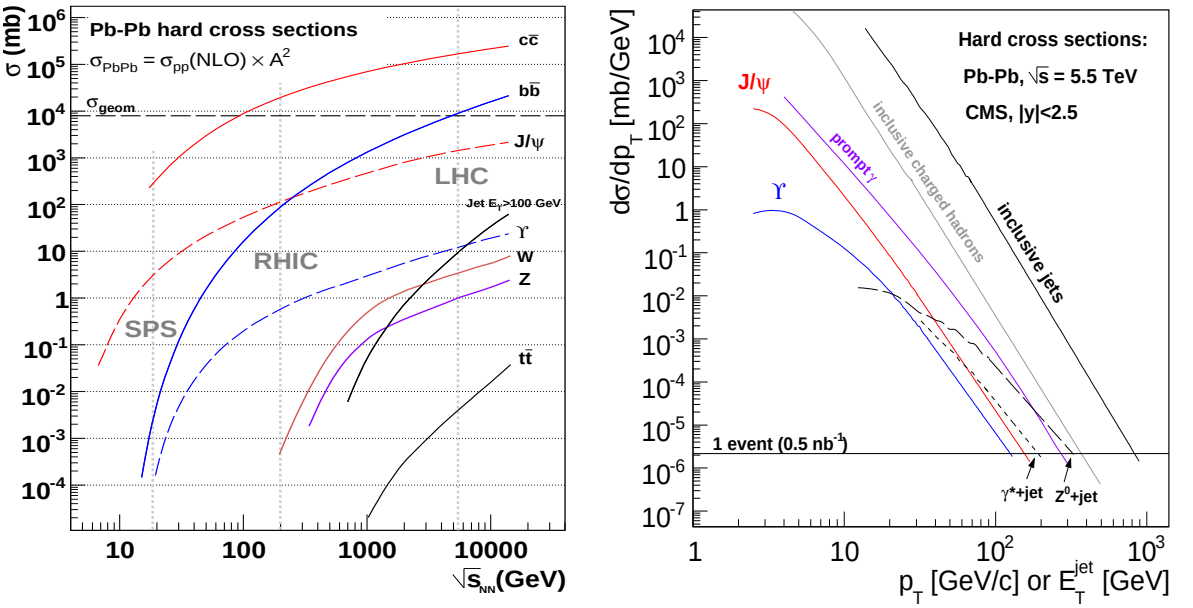

Figure 1. Left: Cross sections for various hard processes ($\sigma^{hard}_{PbPb} = A^2\sigma^{hard}_{pp}$) in Pb-Pb min. bias collisions in the range $\sqrt{s_{NN}} \approx 0.01$–14 TeV. Right: Differential hard cross sections in Pb-Pb at $\sqrt{s_{NN}} = 5.5$ TeV in the CMS acceptance [1].

1. The CMS experiment

CMS is a general purpose experiment at the LHC designed to explore the physics at the TeV energy scale [6]. The CMS detector is a 22 m (length) × 15 m (diameter) apparatus (12 500 tons in weight) featuring a 4 T solenoid surrounding central silicon pixel and microstrip tracking detectors and electromagnetic ($|\eta| < 3$) and hadronic ($|\eta| < 5$) calorimeters. Muon detectors ($|\eta| < 2.4$) are embedded in the flux return iron yoke of the magnet. CMS is the largest acceptance detector at the LHC (Fig. 2) with unique detection capabilities in the very forward hemisphere with the CASTOR ($5.1 < |\eta| < 6.6$) and the Zero-Degree (ZDCs, $|\eta_{neut}| > 8.3$) calorimeters [7]. The detector subsystems have been designed with a resolution and granularity adapted to cope with the extremely high luminosities expected in the p-p running mode ($\mathcal{L} \sim 10^{34}$ cm^{-2}s^{-1} at 14 TeV) with up to 25 simultaneous collisions per bunch crossing. The detector can thus perfectly deal with the large particle multiplicities anticipated for Pb-Pb collisions at 5.5 TeV, where the luminosity is 7 orders of magnitude smaller ($\mathcal{L} \sim 10^{27}$cm^{-2}s^{-1}).

A key aspect of the CMS capabilities for heavy-ion physics – in particular to fully exploit the rare probes available at the LHC – is its unparalleled high-level-trigger (HLT) system running on a filter farm with an equivalent of $O(10^4)$ 1.8 GHz CPU units, yielding few tens of Tflops [8]. The HLT system is powerful enough to run "offline" algorithms on *every single* Pb-Pb event delivered by the level-1 trigger, and select the interesting events while reducing the data stream from an average 3 kHz L1 input/output event rate down to 10–100 Hz written to permanent storage. The resulting enhanced statistical reach for hard probes is a factor of ×20 to ×300 larger, depending on the signal, than for the min-bias (MB) trigger (Section 3).

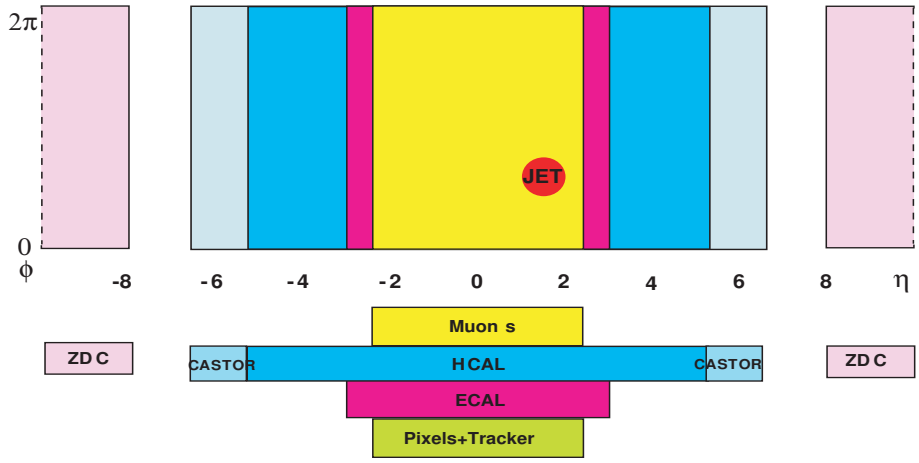

Figure 2. CMS coverage for tracking, calorimetry, and muon identification in pseudo-rapidity (η) and azimuth (ϕ). The size of a jet with cone $R = 0.5$ is also depicted for comparison.

2. Soft observables in Pb-Pb collisions at $\sqrt{s_{NN}}$ = 5.5 TeV

(1) Charged hadron Pb-Pb rapidity density ($dN_{ch}/d\eta$): initial entropy (gluon) density

The charged-particle multiplicity per unit rapidity, $dN_{ch}/d\eta$, is directly related to the entropy density generated in Pb-Pb collisions which in itself fixes the initial global properties of the produced matter. Colour Glass Condensate (CGC) approaches [5], which effectively take into account a reduced initial parton flux in the colliding nuclei, can reproduce the centrality and center-of-mass (c.m.) energy dependences of the bulk A-A hadron production at RHIC. At the LHC, the relevance of low-x QCD effects will be significantly enhanced since the factor of 30 increase in the c.m. energy, implies a similar reduction in the range of typical fractional momenta of the colliding gluons ($x \sim Q/\sqrt{s}$). Current Pb-Pb multiplicities expected at the LHC are $dN/d\eta|_{\eta=0} \approx$ 1200–2000 [9]. Given the excellent granularity of the Si pixel detector (66M channels in total), a hit counting measurement *à la* PHOBOS [10] in the innermost pixel layer is possible with very low occupancies (less than 2%). Figure 3 (left) shows the generated and reconstructed primary hadron multiplicity within $|\eta| < 2.5$ in central Pb-Pb collisions.

(2) Soft hadron spectra (dN/dp_T): medium Equation-of-State (EoS)

Measurement of the bulk pion, kaon and (anti)proton spectra in Pb-Pb at 5.5 TeV and their comparison to hydrodynamical models will provide the first estimates of the conditions characterising the initial- (thermalisation time, baryochemical potential) and final- (freeze-out temperature) states, as well as the first constraints on the EoS of the produced medium.

Despite its large magnetic field, CMS can reconstruct very low p_T tracks down to 0.2 GeV/c – by making use of *just* the three highly segmented layers of the silicon pixel tracker and of its analogue readout – with a modified hit triplet finding algorithm and a (cluster-shape-based) cleaning procedure which reduces the fake rate in high particle density

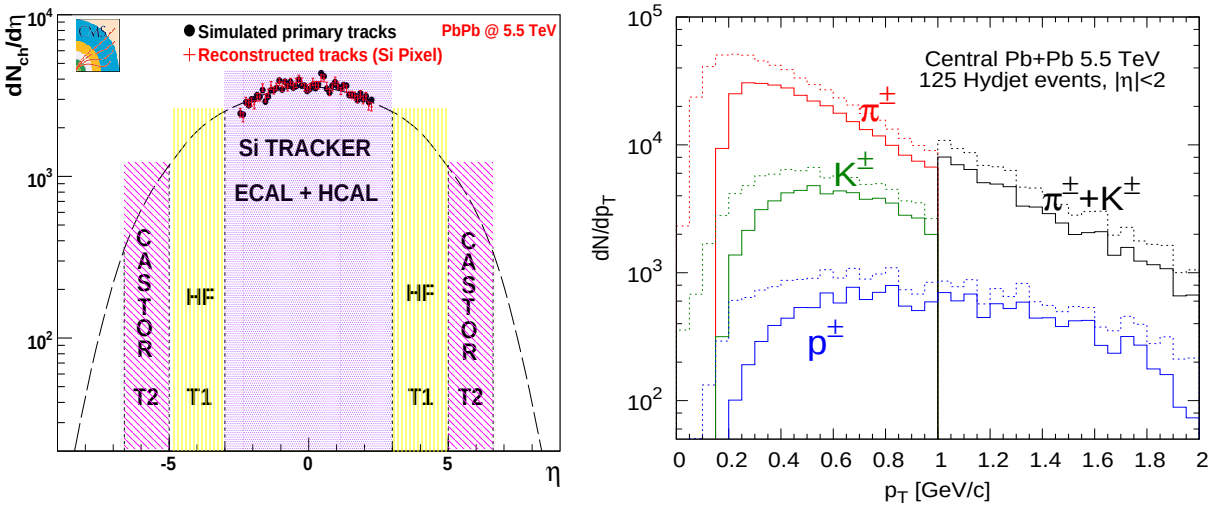

Figure 3. Bulk hadron production in central Pb-Pb collisions at 5.5 TeV [3]. Left: Pseudo-rapidity distribution of primary tracks simulated with HIJING (black dots) compared to the reconstructed hits in the first layer of the Si tracker (red crosses) within $|\eta| < 2.5$. Right: Reconstructed (solid) and generated (HYDJET, dotted) p_T spectra of pions, kaons and protons.

environments [3]. The energy loss of the tracks, dE/dx, can be estimated, in addition, from the charge deposited in the individual pixels of the clusters, providing particle identification in a limited p_T range. Inclusive yields can be extracted up to ≈ 1 GeV/c (2 GeV/c) for pions and kaons (for p, $\bar{\text{p}}$) via Gaussian unfolding of the measured dE/dx distributions. The expected identified hadron p_T spectra in central Pb-Pb collisions are shown in Fig. 3, right.

(3) Elliptic flow (v_2 parameter): medium viscosity

The observation of strong azimuthal anisotropies with respect to the reaction plane, has been one of the highlight results in Au-Au collisions at RHIC. The good agreement of the elliptic flow (v_2) data with *ideal* relativistic hydrodynamics indicates that the produced matter develops a strong collective flow in the first fm/c of the collision and behaves as a "perfect fluid", with a viscosity near a conjectured lower bound [11]. The measurement of the differential v_2 in Pb-Pb collisions at the LHC will be of primary importance to constrain the viscosity of the produced matter and test its liquid-like (or weakly-interacting) properties.

The reaction plane can be independently determined with different CMS detector subsystems using various analysis methods [3, 12]. At central rapidities ($|\eta| < 2.5$) CMS will be able to determine the reaction plane using the tracker and calorimeters, whereas at forward rapidities v_2 will be measured with the HF and CASTOR calorimeters, in a region almost free from non-flow contributions. At beam-rapidity, the ZDCs can provide an independent determination from the directed flow signal (v_1). The expected precision of the reaction-plane measurement will give access to azimuthal anisotropy studies for charged particles (identified or not) in a momentum range from a few hundred MeV/c up to a few hundred GeV/c.

3. Hard observables in Pb-Pb collisions at $\sqrt{s_{NN}}$ = 5.5 TeV

CMS is, by design, very well adapted to detect (reconstruct) high-p_T (high-mass) particles. This section covers various studies that show the capabilities of the detector to measure high-p_T hadrons, full jets, photon-jet processes, and quarkonium production in Pb-Pb collisions.

(4) High-p_T hadron and jet spectra ($R_{AA}(p_T)$, $d^2N_{jet}/d\eta dp_T$): medium transport coefficient

The suppression of inclusive hadron production at high transverse momentum in central Au-Au compared to p-p collisions, has been one of the most important observables at RHIC to study medium-induced parton energy loss. The measured suppression factor (R_{AA}) provides information on the initial gluon density, dN_g/dy, and on the dissipative properties of the medium quantified by its transport coefficient, $\langle\hat{q}\rangle$ [13]. CMS can significantly extend the p_T reach with respect to RHIC, thanks to the large hard cross sections at 5.5 TeV, the large acceptance of its tracking system ($|\eta| < 2.5$), and its high-p_T triggering capabilities. The (complete) silicon tracker has excellent reconstruction performances attaining a 60% (total) efficiency above $p_T > 1$ GeV/c with a fake track rate below 5% for central Pb-Pb. Within $|\eta| < 1$, the p_T resolution is better than 2% up to the highest p_T values reachable. The leading hadron suppression can thus be measured with low uncertainties all the way up to 300 GeV/c, allowing us to clearly discriminate between various model predictions (Fig. 4, left).

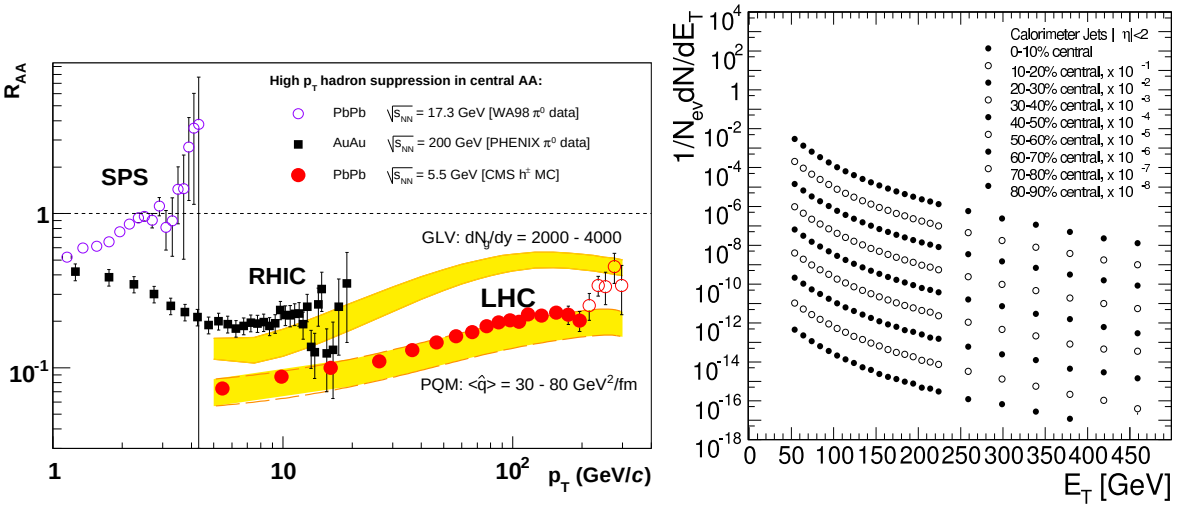

Figure 4. Left: Nuclear modification factor, $R_{AA}(p_T)$, for high-p_T hadrons at CERN-SPS (open dots) and RHIC (squares) compared to CMS pseudo-data (closed circles: MB, open circles: HLT) and to theoretical LHC expectations from GLV [14] (dN_g/dy = 2000–4000) and PQM [15] ($\langle\hat{q}\rangle \approx$ 30–80 GeV^2/fm) models. Right: Inclusive jet E_T distributions in 10 centrality bins expected in CMS for Pb-Pb at 5.5 TeV (0.5 nb^{-1}) using MB- and HLT-triggered data.

Full jet reconstruction in Pb-Pb collisions can be performed in CMS using the ECAL and HCAL calorimeters with an iterative cone algorithm (R = 0.5 cone size) and subtracting the underlying soft background on an event-by-event basis [1]. Jets start to be distinguishable above the background at E_T ~30 GeV and can be fully reconstructed above 75 GeV (efficiency

and purity close to 100%) with a good energy resolution (better than 15%). Figure 4 (right) shows the expected jet E_T spectrum after one month of Pb-Pb running (0.5 nb^{-1}), taking into account High Level Trigger bandwidths and quenching effects as implemented in HYDJET. The large E_T reach, up to 0.5 TeV in central Pb-Pb, will allow us to carry out detailed differential studies of jet quenching phenomena (jet shapes, energy-particle flow within the jet, ...).

(5) Photon-tagged jet production: medium-modified fragmentation functions

The γ-jet (and Z-jet) channel provides a very clean means to determine parton fragmentation functions (FFs) [16] which in turn are very sensitive to the underlying $\langle\hat{q}\rangle$ parameter [17]. Since the prompt γ is not affected by final-state interactions, its transverse energy ($E_{\rm T}^{\gamma}$) can be used as a proxy of the away-side parton energy ($E_{\rm T}^{\rm jet} \approx E_{\rm T}^{\gamma}$) *before* any jet quenching has taken place in the medium. The FF, i.e. the distribution of hadron momenta, $1/N_{jets}\, dN/dz$, relative to that of the parent parton $E_{\rm T}^{\rm jet}$, can be constructed using $z = p_T/E_{\rm T}^{\gamma}$ or, similarly, $\xi = -\ln z = \ln(E_{\rm T}^{\gamma}/p_T)$, for all particles with momentum p_T associated with the jet.

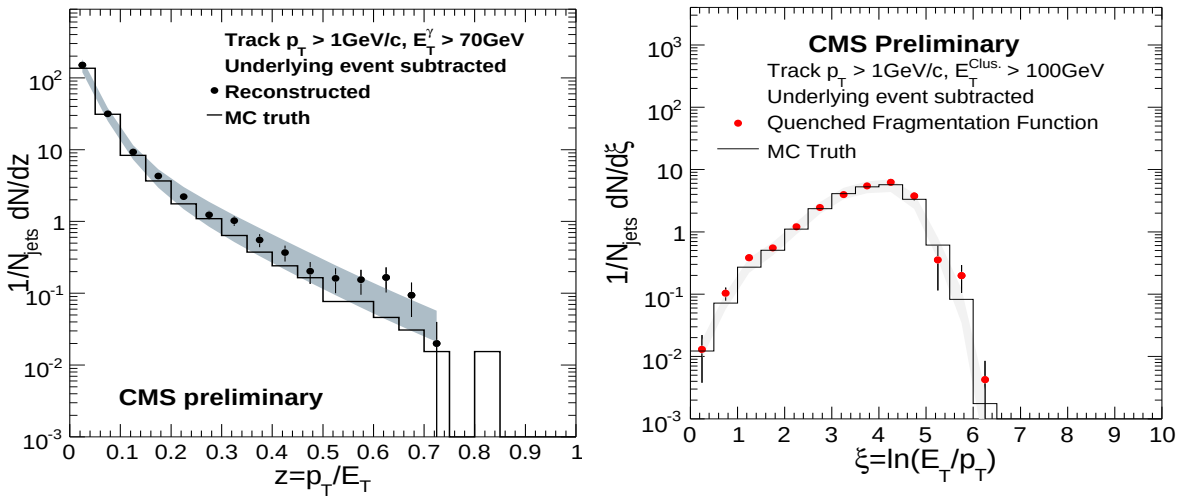

Figure 5. Generated (histogram) and reconstructed (points and error band) fragmentation functions as a function of z (left) and ξ (right) for quenched partons, obtained in γ–jet events with $E_{\rm T}^{\gamma} > 70$ GeV in central Pb-Pb at 5.5 TeV (statistical errors correspond to 0.5 nb^{-1}) [2].

Full CMS simulation-reconstruction studies of the γ-jet channel have been carried out, where the isolated γ is identified in ECAL ($R_{isol} = 0.5$), the away-side jet *axis* ($\Delta\phi_{\gamma-jet} > 3$ rad) is reconstructed in ECAL+HCAL, and the momenta of hadrons around the jet-axis ($R_{jet} < 0.5$) are measured in the tracker [2]. A total of 4300 γ-jet events are expected in one Pb-Pb year at the nominal luminosity (according to PYTHIA simulations scaled by the Glauber nuclear overlap). The obtained FFs for photon-jet events with $E_{\rm T}^{\gamma} > 70$ GeV — after subtraction of the underlying-event tracks using a R = 0.5 cone *transverse* to the jet — are shown in Fig. 5 for central Pb-Pb. Medium modified FFs are measurable with high significance (the systematic uncertainties being dominated by the low jet reconstruction efficiency for $E_{\rm T}^{\rm jet} = 30$–70 GeV) in the ranges $z < 0.7$ or $0.2 < \xi < 5$.

(6) Quarkonium production: critical energy density

Studies of quarkonium production in Pb-Pb at the LHC will provide crucial information on the thermodynamical state of the QCD medium formed in these reactions. Lattice calculations can predict, in principle, the expected step-wise "melting" pattern of the different $Q\overline{Q}$ states due to colour screening as a function of energy density. The Υ, accessible for the first time with large statistics at the LHC, is expected to survive up to 4 times the critical QCD temperature and, thus, suppression of the $b\overline{b}$ ground state would be indicative of medium temperatures around 1 GeV.

CMS can reconstruct the $c\overline{c}$ and $b\overline{b}$ resonances via their dimuon decay channel with very high efficiencies ($\sim 80\%$) and purities ($\sim 90\%$), and the best LHC mass resolution: 54 MeV/c^2 at the Υ mass, in the central barrel ($|\eta| < 0.8$). The Υ states can be measured all the way down to $p_T = 0$ GeV/c with acceptances between 15% and 40%. The large aperture of the muon detectors and the precise tracking result in a very good separation between the $Q\overline{Q}$ states in the dimuon mass distributions, with high statistics and good signal to background ratios (Fig. 6). In the absence of suppression, after one month of Pb-Pb running (0.5 nb^{-1}) CMS will collect $1.8\,10^5$ J/ψ and $2.5\,10^4$ Υ, enough to compare central and peripheral Pb-Pb collisions, and to carry out differential studies (dN/dy, dN/dp_T) that will help to clarify the mechanisms behind the production (and suppression) of $Q\overline{Q}$ states in high-energy nucleus-nucleus collisions.

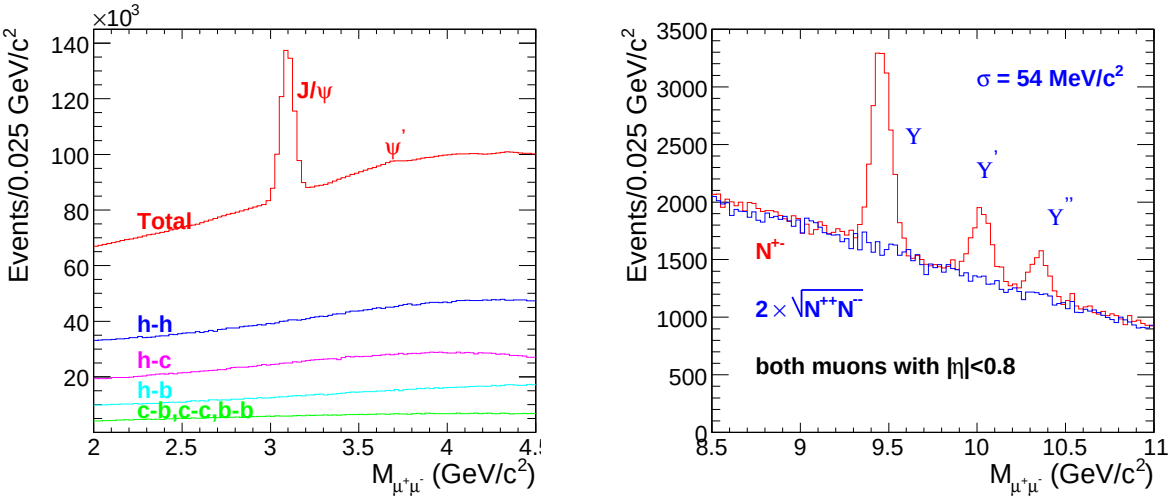

Figure 6. Full simulation studies of quarkonia production in Pb-Pb at 5.5 TeV ($dN_{ch}/d\eta|_{\eta=0} = 2500$). Left: Dimuon mass distributions within $|\eta| < 2.4$ (the h, c and b backgrounds stand for decay muons from $\pi + K$, charm, and bottom, resp.). Right: Invariant mass spectra of opposite-sign and like-sign muon pairs (within $|\eta| < 0.8$) in the Υ mass region.

(7) Exclusive Υ photoproduction: low-x parton distribution functions (PDFs)

The strong electromagnetic fields (equivalent fluxes of quasi-real photons) in ultraperipheral heavy-ion collisions (UPCs), where both nuclei pass at distances $R \gtrsim 20$ fm, can be used to study various $\gamma\gamma$ and γ-nucleus processes up to c.m. energies $W_{\gamma\gamma}^{max} \approx 160$ GeV and

$W_{\gamma A}^{max} \approx 1$ TeV [18]. The Bjorken-x values probed in quarkonium photoproduction processes (γPb$\rightarrow \Upsilon$Pb) can be as low as $x \sim 10^{-4}$ where the nuclear PDFs, in particular the gluon one, have very large uncertainties (Fig. 7, left).

Full simulation+reconstruction studies show that CMS can measure $\Upsilon \rightarrow e^+e^-$, $\mu^+\mu^-$ within $|\eta| < 2.5$, in UPCs tagged with neutrons detected in the ZDCs. Figure 7 (right) shows the reconstructed $dN/dm_{\mu^+\mu^-}$ around the Υ mass. The expected total yield of $\sim$400 Υ/year in the dielectron and dimuon channels will allow us to carry out differential (p_T,η) studies to help constrain the low-x gluon density in the Pb nucleus.

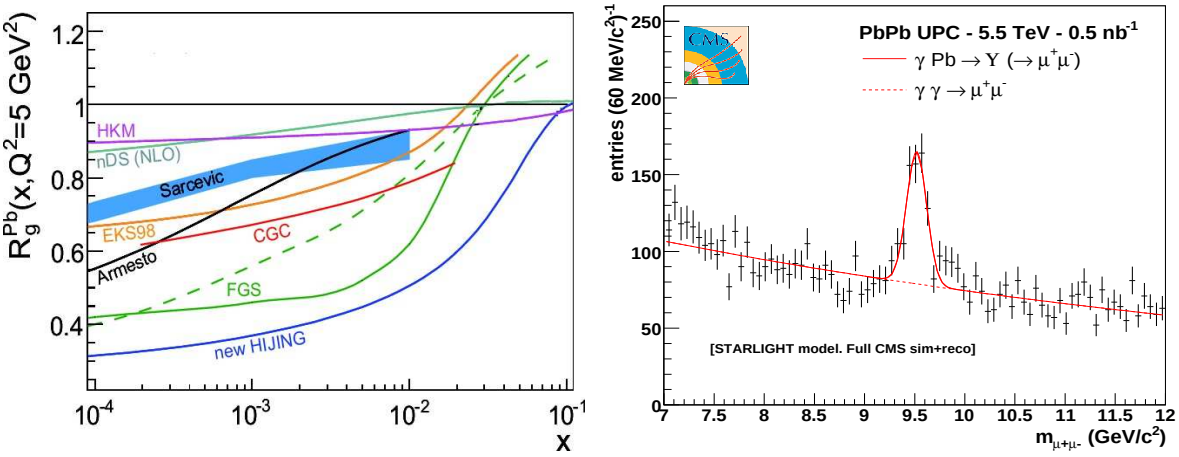

Figure 7. Left: Pb-over-proton gluon densities ratio as a function of x at fixed $Q^2 = 5$ GeV^2 from various PDF fits. Right: Expected $\mu^+\mu^-$ invariant mass distribution from γPb$\rightarrow \Upsilon$Pb* ($\Upsilon \rightarrow \mu^+\mu^-$, signal) and $\gamma\gamma \rightarrow \mu^+\mu^-$ (background) in UPCs triggered with the ZDC.

Acknowledgments. Supported by 6th EU Framework Programme MEIF-CT-2005-025073.

References

[1] d'Enterria D (ed.) *et al.* [CMS Collaboration] 2007 J. Phys. G **34** 2307.
[2] Loizides C [CMS Collaboration] 2008, these Proceeds., arXiv:0804.3679
[3] Sikler F [CMS Collaboration] 2008, these Proceeds., arXiv:0805.0809
[4] Dutta D [CMS Collaboration] 2008, these Proceeds., arXiv:
[5] Venugopalan R 2008, these Proceeds.
[6] de Roeck A (ed.) *et al.* [CMS Collaboration] 2007, *J. Phys. G: Nucl. Phys.* **34** 995.
[7] Albrow M *et al.* [CMS/TOTEM Collaborations] 2006, CERN-LHCC-2006-039/G-124
[8] Roland G [CMS Collaboration] 2007, J. Phys. G **34** S733
[9] Armesto N 2008, these Proceeds., arXiv:0804.4158 [hep-ph].
[10] Back B B *et al.* [PHOBOS Collaboration] 2000, Phys. Rev. Lett. **85** 3100
[11] Kovtun P, Son D T and Starinets A O 2005, Phys. Rev. Lett. **94** 111601
[12] Eyyubova G [CMS Collaboration] 2008, QM'08 poster proceeds.
[13] Casalderrey-Solana J and Salgado C A 2007, Acta Phys. Polon. B **38** 3731.
[14] Vitev I, Gyulassy M 2002, Phys. Rev. Lett. 89 252301.
[15] Loizides C 2007, Eur. Phys. J. C **49** 339
[16] Arleo F *et al.* 2004, JHEP **0411** 009
[17] Armesto N *et al.* 2008, JHEP **0802** 048
[18] Baltz A *et al.* 2008, Phys. Rept. **458** 1